ChemComm

www.rsc.org/chemcomm

COMMUNICATION

High aspect ratio γ-MnOOH nanowires for high performance rechargeable nonaqueous lithium–oxygen batteries†

Leilei Zhang,[ab] Xinbo Zhang,*[a] Zhongli Wang,[a] Jijing Xu,[a] Dan Xu[a] and Limin Wang*[a]

High aspect ratio γ-MnOOH nanowires (MNWs) are synthesized by a simple one-step hydrothermal method and used as catalysts in rechargeable nonaqueous lithium–oxygen batteries. When the nanowires are employed, great improvements in discharge capacity, cycle stability, and rate retention are obtained, which are attributed to the high catalyst efficiency and the cathode porosity.

Rechargeable lithium–oxygen (Li–O$_2$) batteries have attracted worldwide interest due to their high energy density of 5200 W h kg^{-1}, which is 5–10 times greater than that of conventional lithium intercalation compound based batteries such as LiCoO$_2$.[1] This high energy density endows Li–O$_2$ batteries with great promise for electric vehicle and other high energy storage applications. However, many challenges must be overcome before they can be considered further for practical applications, including low electrolyte stability, sluggish kinetics, poor rate capability and short cycle life.[2]

The cathode is the bottle-neck of a nonaqueous Li–O$_2$ battery, wherein the terribly sluggish oxygen reduction/evolution reaction (ORR/OER) kinetics not only increases the overpotential, but also causes pitiful rechargeability and low rate capability. On the other hand, the solid discharge products are insoluble and thus precipitate in the pores of cathode, leading to low capacity and poor cycle performance. Therefore, it is vital to develop a porous cathode that is also a highly effective catalyst. To this end, intensive research efforts have been devoted to addressing the challenge by incorporating metal oxides,[2a,c,3] metal nitrides,[2b] phthalocyanine compounds,[1a,2d,e] or noble metals,[4] *etc.*, with different morphologies involving nanoparticles or nanospheres,[2b,3c,4b] nanowires (NWs),[3b,e] and nanosheets[3a,g] *etc.* as catalysts into the O$_2$ electrode. Despite the fact that these catalysts have improved the battery performance to some extent, the development of Li–O$_2$ batteries is still in its infancy period and great efforts are urgently needed.

Manganite (MnOOH) materials are important precursors[5] for other manganese oxides and active electrocatalysts for the ORR in an alkaline electrolyte.[6] Suib *et al.* have reported γ-MnOOH particles with a discharge capacity of 2200 mA h g^{-1} but a lack of cycle stability.[3f] To the best of our knowledge, we are the first to use γ-MnOOH as a catalyst for a rechargeable Li–O$_2$ battery. Herein, high aspect ratio MNWs have been successfully synthesized through a simple one-step hydrothermal process using only potassium permanganate (KMnO$_4$) and polyvinylpyrrolidone (PVP). The MNWs show high catalytic activity for the ORR and OER in nonaqueous electrolyte and, even more importantly, display excellent performance in a Li–O$_2$ battery.

PVP as a surfactant is widely used in nanomaterial synthesis.[7] However, as far as we know, this is the first time high aspect ratio MNWs have been synthesized using only KMnO$_4$ and PVP, which is the least reactants reported to date (detailed preparation processes are given in ESI†). Fig. 1a shows the XRD pattern of the synthesized product. All diffraction peaks match well with the monoclinic γ-MnOOH structure ($P2_1/c$, space group 14, cell = 5.3 × 5.278 × 5.307 ⟨90 × 114.36 × 90⟩, JCPDF No. 41-1379). The two obvious sharp peaks can be indexed to the (11–1) plane, suggesting good crystallinity and
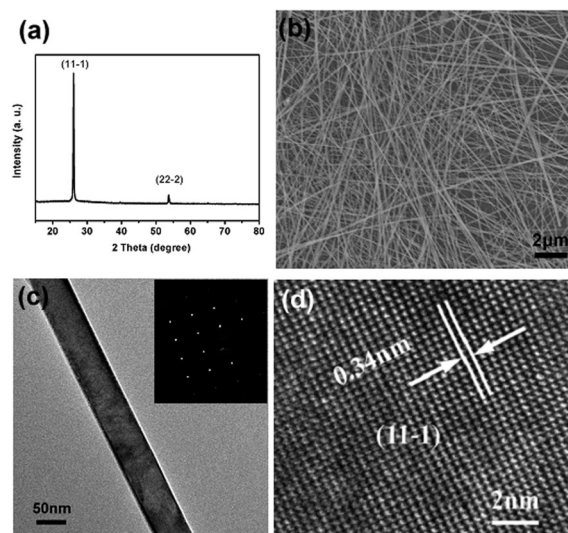

Fig. 1 (a) An XRD pattern, (b) SEM image, (c) TEM image, SAED pattern (inset c), and (d) HRTEM image of the MNWs.

[a] *State Key Laboratory of Rare Earth Resource Utilization, Changchun Institute of Applied Chemistry, Chinese Academy of Sciences, Changchun, 130022, Jilin, China. Fax: 086 431 85262235; Tel: 086 431 85262235; E-mail: xbzhang@ciac.jl.cn; 086 431 85262447; 086 431 85262447; lmwang@ciac.jl.cn*
[b] *Graduate University of Chinese Academy of Sciences, Beijing 100049, China*
† Electronic supplementary information (ESI) available: Experimental details and supplementary figures. See DOI: 10.1039/c2cc33933a

homogenous orientation of the prepared sample. Typical scanning electron microscopy (SEM) (Fig. 1b) and transmission electron microscopy (TEM) (Fig. 1c) images clearly show a one-dimensional (1D) NW morphology of the as-synthesized γ-MnOOH, which exhibits smooth side edges with an average diameter of 60 nm and length of up to tens of microns. The microstructure of the product is further investigated by the means of a selected-area electron diffraction (SAED) pattern and high resolution TEM (HRTEM). The SEAD pattern (Fig. 1c, inset) indicates the single crystal nature. The HRTEM image enables a clear view of lattice fringes which are shown in Fig. 1d. The well-resolved lattice fringes give an interplanar spacing of 0.34 nm, corresponding with the distance of the (11–1) plane of γ-MnOOH. This indicates that the growth of the MNWs is along the [11–1] direction and the results agree well with what the XRD pattern is showing.

Cyclic voltammetry (CV) was employed to investigate the ORR and OER activity of the synthesized MNWs in nonaqueous electrolyte. The CV curves of both MNWs and Kejtenblack carbon (KB) tested in argon show no obvious cathodic or anodic peak current (Fig. S1†), indicating their stability in the electrolyte at the voltage range of 2.0–4.4 V. When performed in an O_2 atmosphere, as shown in Fig. 2a, the MNWs exert a higher ORR voltage and an obvious OER peak, and the absolute peak current values are significantly larger than that of KB. These advantages demonstrate promising ORR and OER activities for MNWs as catalysts in nonaqueous Li–O_2 batteries.

Inspired by the superior catalytic activity, we further examined the MNWs performance in a nonaqueous Li–O_2 battery. Note that all the results related to specific capacities are normalized with respect to the mass of the carbon in the electrode. Propylene carbonate (PC) was used as the electrolyte firstly because in PC the effect of catalysts can be compared well with former reports.[3b,e,h,8] The discharge and charge voltages can be influenced greatly by the MNWs used in the O_2 electrode. As shown in Fig. 2b, the discharge voltage of MNWs/KB is slightly higher than that of pure KB by $\sim$30 mV. While charging, the voltage is substantially lower (by 300 mV) than

that of pure KB. The charge voltage is around 3.8 V, which is as low as PtAu (3.4–3.8 V),[4b] and lower than most reported catalysts such as MnO_x/C ($\sim$4.2 V),[3h] α-MnO_2 NWs,[3b] Co_3O_4 ($\sim$4.0 V)[2a] etc. Moreover, the background measurement during charging demonstrates that the low charge voltage is not the result of electrolyte decomposition which is 4.5 V (Fig. S2†). The variation of the discharge capacity with the cycle number at 0.05 mA cm^{-2} is presented in Fig. 2c. It is evident that MNWs/KB have a much higher capacity than pure KB. The initial discharge capacity is 2693 mA h g^{-1}, which then rises slightly on the second cycle, and fluctuates between 2600 and 2400 mA h g^{-1} on the following cycles. Although it drops down to 1947 mA h g^{-1} after 10 cycles, the capacity retention is still as high as 72.3%. By contrast, the initial discharge capacity with pure KB is only 1888 mA h g^{-1}, 30% lower than that of MNWs/KB, and it drops seriously to 469 mA h g^{-1} on the 10th cycle with a capacity retention of just 24.8%. From the typical discharge/charge profiles shown in Fig. S3†, we can see that both the discharge and charge plateaus of MNWs/KB are well preserved upon cycling. But there are nearly no discharge or charge plateaus for pure KB except in the first discharge. The cycle stability of the MNWs/KB is better than that reported by Bruce,[3b] and the capacity and cycling performance hold an absolute superiority over other reports to date. Reports on cycles at a deep discharge are currently rare, especially with the capacity above 2000 mA h g^{-1}. When we restrict the capacity to 1000 mA h g^{-1}, excellent capacity reversibility can also be obtained after 20 cycles, as illustrated in Fig. S4.†

The rate capabilities of the MNWs/KB and pure KB are shown in Fig. 2d (the detailed discharge curves are given in Fig. S5†). The specific capacity and the discharge voltage decrease with the increased current density, since the electrochemical polarization becomes much more significant at higher current densities.[9] On the other hand, the slow dissolution rate of Li metal into the electrolyte and the low oxygen solubility and diffusivity of the PC electrolyte[10] also play a key part in limiting the discharge reaction at higher current rates. However, the capacity retention is still as high as 48% at the current density of 0.15 mA cm^{-2}, demonstrating a high rate performance when compared with that of pure KB, which is only 11%.

To further investigate the possible reasons why the MNWs improve the cycle and rate capacities greatly, we compare the SEM images of O_2 electrodes before and after discharge. As shown in Fig. 3a, the MNWs disperse disorderly, confusedly and interlace together. When discharging, the insoluble products deposit and build up on the MNWs, the carbons and in the void volume. After discharge, there is still a lot of free space within the electrode (Fig. 3b). While, in the pure KB electrode, the discharge products only deposit on KB, and the surface of electrode is tightly covered by the aggregated products (Fig. S6†). From the above observation, we speculate that in addition to the inherently high ORR and OER activities of the MNWs, the electrode structure of the MNWs should also play an important role. The long MNWs can form a skeleton to support KB particles, making the electrode loose and porous. This porosity can not only provide much space for discharge products, but also promote the flow of gases and infiltration of the electrolyte, and eventually, improve the
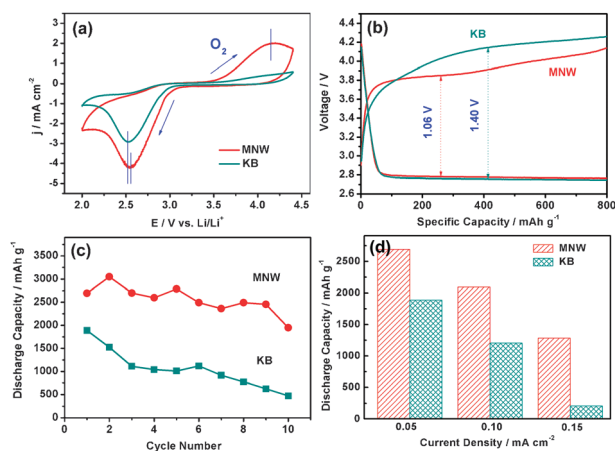

Fig. 2 (a) CV curves at a scan rate of 20 mV s^{-1}; (b) discharge/charge curves with a restricting capacity at a current density of 100 mA g^{-1}; (c) variation of discharge capacity with cycle number at a current density of 0.05 mA cm^{-2}; (d) the discharge capacities at different current densities.
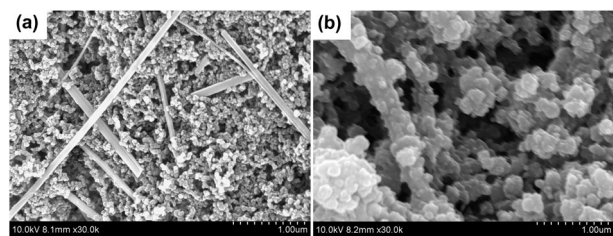
Fig. 3 SEM images of the MNWs cathode (a) before and (b) after discharge.

capacity and cyclability greatly. The advantageous combination of the intrinsically high catalytic activity and unique structure is responsible for the superior performance of the $Li–O_2$ cells. To further confirm the above speculation, we synthesized γ-MnOOH NRs (MNRs) with a 50 nm diameter and less than 1 μm in length (the aspect ratio is less than 20, shown in Fig. S7a and S7b†). These MNRs are not long enough to interlace and form a porous skeleton so that as expected, the capacity of the MNRs is lower than that of the MNWs (Fig. S7c and Fig. S8†). This might be a main reason why 1D materials perform better in former reports.[11,3b,e]

Although the MNWs show an outstanding performance in $Li–O_2$ batteries with PC as the electrolyte, PC is a controversial electrolyte in most recent reports because of its decomposition and byproducts.[12] However, we believe that the MNWs will display an excellent performance in other electrolytes due to their outstanding catalytic activity and forming of a porous skeleton electrode. We extended the experiment to a dimethoxyethane (DME) based electrolyte since it is comparatively stable and the diffusion of O_2 is faster.[13] As expected, the discharge capacity and rate capacity improved greatly (see Fig. S9† and Table S1† for details).

In summary, high aspect ratio MNWs have been successfully prepared by a simple one-step hydrothermal method. Applying the MNWs as catalysts in a $Li–O_2$ battery, the MNWs form a skeleton making the electrode loose and porous to provide excess void space, benefiting the storage of discharge products, flow of gases, and soak of the electrolyte. $Li–O_2$ batteries with this highly catalytic porous cathode show an outstanding performance both in PC and DME based electrolytes.

Notes and references

1 (a) K. M. Abraham and Z. Jiang, *J. Electrochem. Soc.*, 1996, **143**, 1–5; (b) M. Armand and J. M. Tarascon, *Nature*, 2008, **451**, 652–657; (c) T. Ogasawara, A. Debart, M. Holzapfel, P. Novak and P. G. Bruce, *J. Am. Chem. Soc.*, 2006, **128**, 1390–1393; (d) P. G. Bruce, S. A. Freunberger, L. J. Hardwick and J. M. Tarascon, *Nat. Mater.*, 2012, **11**, 19–29.

2 (a) A. Débart, J. Bao, G. Armstrong and P. G. Bruce, *J. Power Sources*, 2007, **174**, 1177–1182; (b) S. Dong, X. Chen, K. Zhang, L. Gu, L. Zhang, X. Zhou, L. Li, Z. Liu, P. Han, H. Xu, J. Yao, C. Zhang, X. Zhang, C. Shang, G. Cui and L. Chen, *Chem. Commun.*, 2011, **47**, 11291–11293; (c) H. Minowa, M. Hayashi, M. Takahashi and T. Shodai, *Electrochemistry*, 2010, **78**, 353–356; (d) S. S. Zhang, X. Ren and J. Read, *Electrochim. Acta*, 2011, **56**, 4544–4548; (e) X. Ren, S. S. Zhang, D. T. Tran and J. Read, *J. Mater. Chem.*, 2011, **21**, 10118–10125.

3 (a) S. Ida, A. K. Thapa, Y. Hidaka, Y. Okamoto, M. Matsuka, H. Hagiwara and T. Ishihara, *J. Power Sources*, 2012, **203**, 159–164; (b) A. Débart, A. J. Paterson, J. Bao and P. G. Bruce, *Angew. Chem., Int. Ed.*, 2008, **47**, 4521–4524; (c) G. Zhang, J. Zheng, R. Liang, C. Zhang, B. Wang, M. Au, M. Hendrickson and E. Plichta, *J. Electrochem. Soc.*, 2011, **158**, A822–A827; (d) L. Jin, L. Xu, C. Morein, C. h. Chen, M. Lai, S. Dharmarathna, A. Dobley and S. L. Suib, *Adv. Funct. Mater.*, 2010, **20**, 3373–3382; (e) Y. M. Cui, Z. Y. Wen and Y. Liu, *Energy Environ. Sci.*, 2011, **4**, 4727–4734; (f) V. M. B. Crisostomo, J. K. Ngala, S. Alia, A. Dobley, C. Morein, C. H. Chen, X. Shen and S. L. Suib, *Chem. Mater.*, 2007, **19**, 1832–1839; (g) J. X. Li, N. Wang, Y. Zhao, Y. H. Ding and L. H. Guan, *Electrochem. Commun.*, 2011, **13**, 698–700; (h) H. Cheng and K. Scott, *J. Power Sources*, 2010, **195**, 1370–1374.

4 (a) Y. C. Lu, H. A. Gasteiger and Y. Shao-Horn, *J. Am. Chem. Soc.*, 2011, **133**, 19048–19051; (b) Y. C. Lu, Z. C. Xu, H. A. Gasteiger, S. Chen, K. Hamad Schifferli and Y. Shao-Horn, *J. Am. Chem. Soc.*, 2010, **132**, 12170–12171; (c) A. K. Thapa and T. Ishihara, *J. Power Sources*, 2011, **196**, 7016–7020.

5 W. Chen, N. Wang, L. Liu, Y. Cui, X. Cao, Q. Chen and L. Guo, *Nanotechnology*, 2009, **20**, 445601–445608.

6 W. Sun, A. Hsu and R. R. Chen, *J. Power Sources*, 2011, **196**, 627–635.

7 (a) H. Jiang, T. Zhao, J. Ma, C. Y. Yan and C. Z. Li, *Chem. Commun.*, 2011, **47**, 1264–1266; (b) S. Preciado Flores, D. Wang, D. A. Wheeler, R. Newhouse, J. K. Hensel, A. Schwartzberg, L. Wang, J. Zhu, M. Barboza Flores and J. Z. Zhang, *J. Mater. Chem.*, 2011, **21**, 2344–2350.

8 X. H. Yang, P. He and Y. Y. Xia, *Electrochem. Commun.*, 2009, **11**, 1127–1130.

9 (a) D. Zhang, Z. Fu, Z. Wei, T. Huang and A. Yu, *J. Electrochem. Soc.*, 2010, **157**, A362–A365; (b) Y. Li, J. Wang, X. Li, J. Liu, D. Geng, J. Yang, R. Li and X. Sun, *Electrochem. Commun.*, 2011, **13**, 668–672.

10 (a) J. Read, K. Mutolo, M. Ervin, W. Behl, J. Wolfenstine, A. Driedger and D. Foster, *J. Electrochem. Soc.*, 2003, **150**, A1351–A1356; (b) Y. C. Lu, D. G. Kwabi, K. P. C. Yao, J. R. Harding, J. Zhou, L. Zuin and Y. Shao-Horn, *Energy Environ. Sci.*, 2011, **4**, 2999–3007.

11 J. Wu, H. W. Park, A. Yu, D. Higgins and Z. Chen, *J. Phys. Chem. C*, 2012, **116**, 9427–9432.

12 (a) S. A. Freunberger, Y. Chen, Z. Peng, J. M. Griffin, L. J. Hardwick, F. Barde, P. Novak and P. G. Bruce, *J. Am. Chem. Soc.*, 2011, **133**, 8040–8047; (b) R. Black, S. H. Oh, J. H. Lee, T. Yim, B. Adams and L. F. Nazar, *J. Am. Chem. Soc.*, 2012, **134**, 2902–2905; (c) J. Xiao, J. Hu, D. Wang, D. Hu, W. Xu, G. L. Graff, Z. Nie, J. Liu and J. G. Zhang, *J. Power Sources*, 2011, **196**, 5674–5678.

13 (a) B. D. McCloskey, R. Scheffler, A. Speidel, D. S. Bethune, R. M. Shelby and A. C. Luntz, *J. Am. Chem. Soc.*, 2011, **133**, 18038–18041; (b) J. Read, *J. Electrochem. Soc.*, 2006, **153**, A96–A100.